Supplementary information

Hybrid $MoSe_2$-indocyanine green nanosheets as a high-efficient phototheranostic agent for photoacoustic imaging guided photothermal cancer therapy

Jingqin Chen,[ab] Xueshen Li,[a] Xiaoyang Liu,[a] Huixiang Yan,[a] Zhihua Xie,[a] Zonghai Sheng,[c] Xiaojing Gong,[a] Lidai Wang,[d] Xin Liu,[c] Peng Zhang,[e] Hairong Zheng,[c] Liang Song,[a] and Chengbo Liu, *[a]

[a] *Research Laboratory for Biomedical Optics and Molecular Imaging, Shenzhen Key Laboratory for Molecular Imaging, Institute of Biomedical and Health Engineering, Shenzhen Institutes of Advanced Technology, Chinese Academy of Sciences, Shenzhen 518055, China.*

[b] *Shenzhen College of Advanced Technology, University of Chinese Academy of Sciences, Shenzhen 518055, China.*

[c] *Paul C. Lauterbur Research Center for Biomedical Imaging, Institute of Biomedical and Health Engineering, Shenzhen Institutes of Advanced Technology, Chinese Academy of Sciences, Shenzhen 518055, China.*

[d] *Prof. L. Wang*

Department of Mechanical and Biomedical Engineering, City University of Hong Kong, 83 Tat Chee Ave, Kowloon, Hong Kong SAR, China.

[e] *Translational Medicine R&D Center, Institute of Biomedical and Health Engineering, Shenzhen Institutes of Advanced Technology, Chinese Academy of Sciences, Shenzhen 518055, China.*

* Corresponding author: C Liu

E-mail: cb.liu@siat.ac.cn. Tel.: +86 (755) 8639-2240

Figure S1

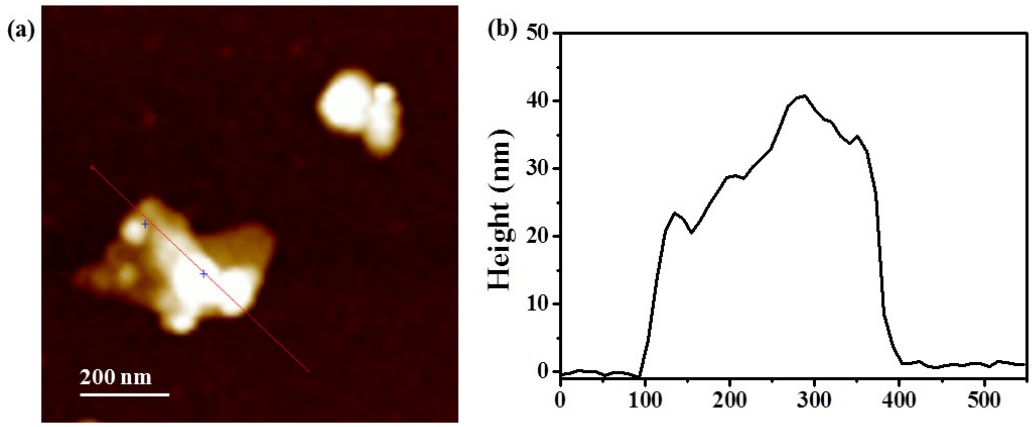

Figure S1 The AFM image and height of bulk $MoSe_2$.

Figure S2

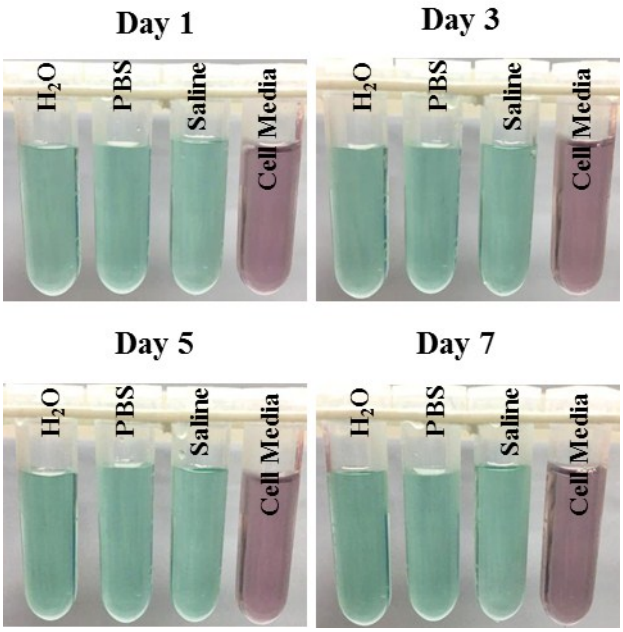

Figure S2 The images of $sMoSe_2$-ICG NSs in water, PBS, saline and cell media at day 1, day 3, day 5 and day 7, respectively.

Figure S3

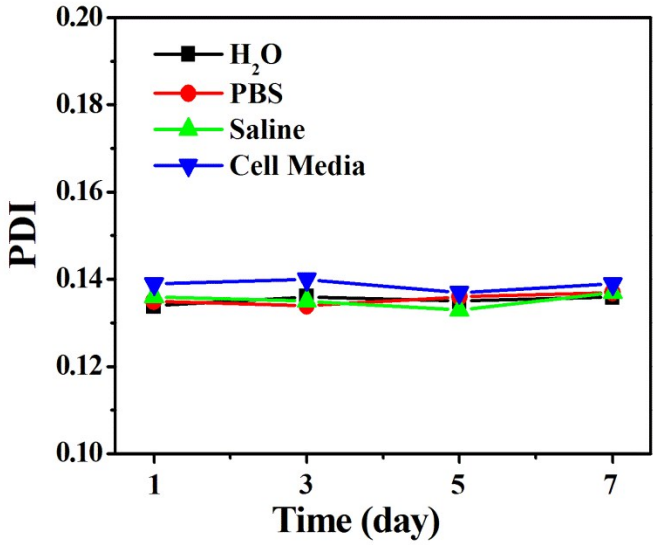

Figure S3 The polydispersity index (PDI) of $sMoSe_2$-ICG NSs in water, PBS, saline and cell media at day 1, day 3, day 5 and day 7, respectively.

Figure S4

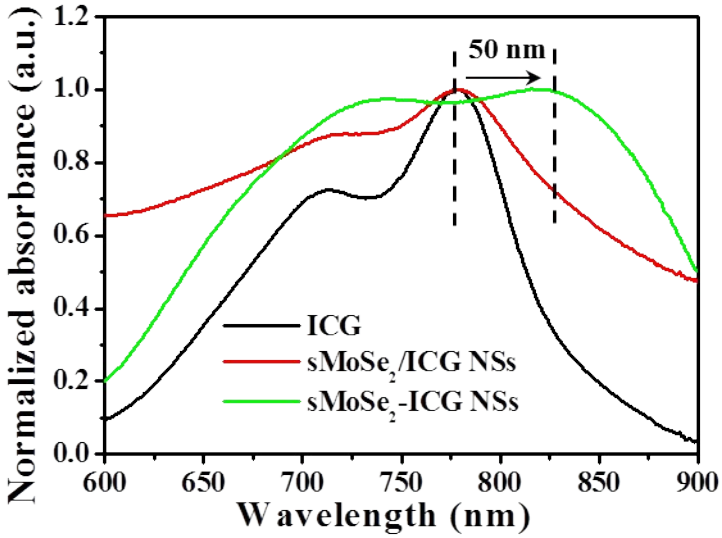

Figure S4 The normalized absorbance spectra of ICG, $sMoSe_2$/ICG NSs and $sMoSe_2$-ICG NSs.

Figure S5

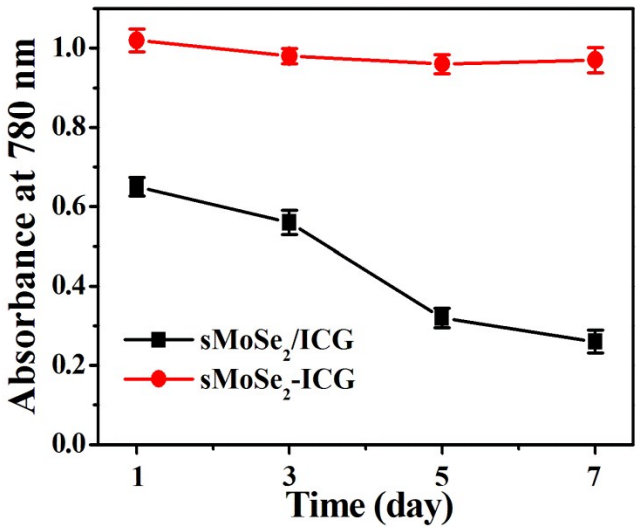

Figure S5 The absorbance of $sMoSe_2$/ICG NSs and $sMoSe_2$-ICG NSs in dialyzate at day 1, day 3, day 5 and day 7, respectively.

Figure S6

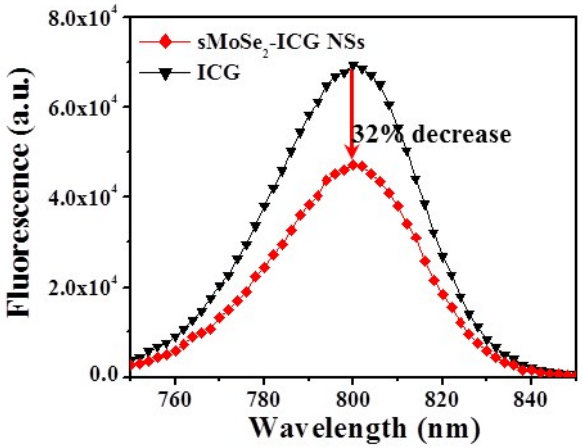

Figure S6 The fluorescence spectra of free ICG and $sMoSe_2$-ICG NSs.

Figure S7

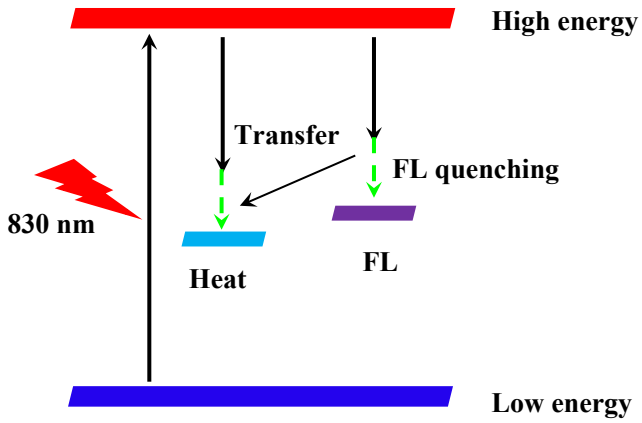

Figure S7 The scheme of energy assignment of sMoSe$_2$-ICG NSs under 830 nm laser irradiation. FL: fluorescence.

Figure S8

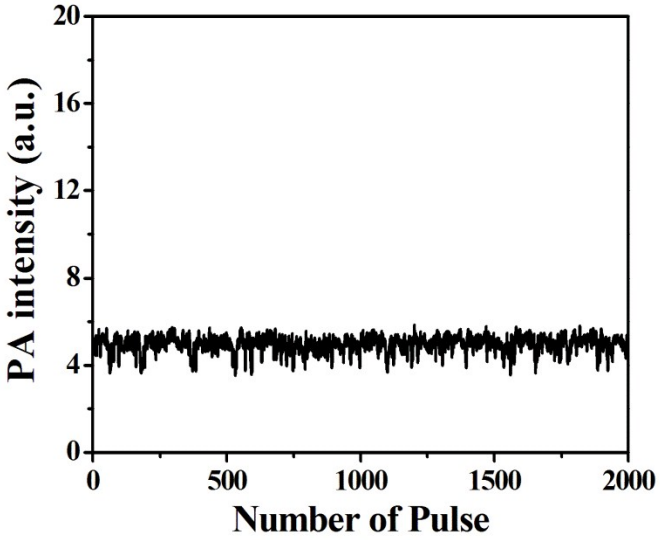

Figure S8 The photostability of $sMoSe_2$-ICG NSs. There was no obvious PA signal attenuation after exposure to 2000 laser pulses (6 mJ/cm^2). PA: photoacoustic.

Figure S9

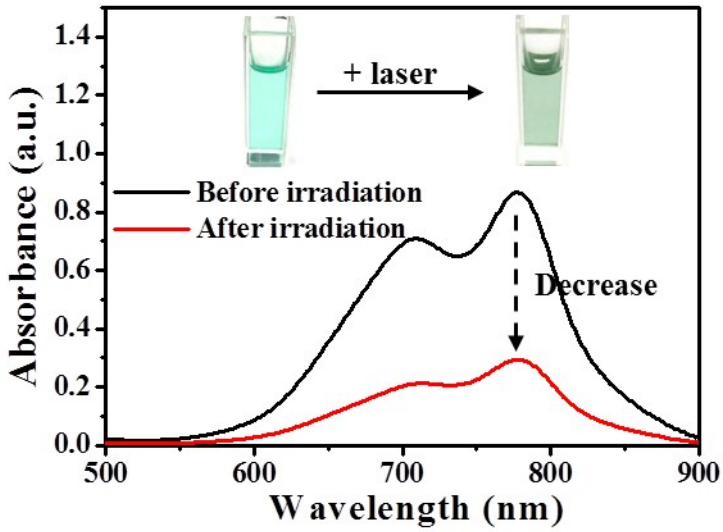

Figure S9 Absorption spectra of free indocyanine green (ICG) solutions before and after 808 nm laser irradiation at a power density of 0.5 W/cm^2 for 5 min; insets are photographs of the ICG solutions before (left) and after (right) laser irradiation.

Figure S10

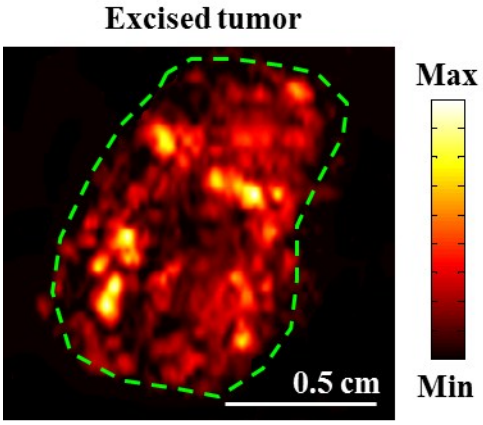

Figure S10 The PA MAP image of excised tumor at 24 h post-injection of sMoSe$_2$-ICG NSs. PA: photoacoustic; MAP: maximum amplitude projection.

Figure S11

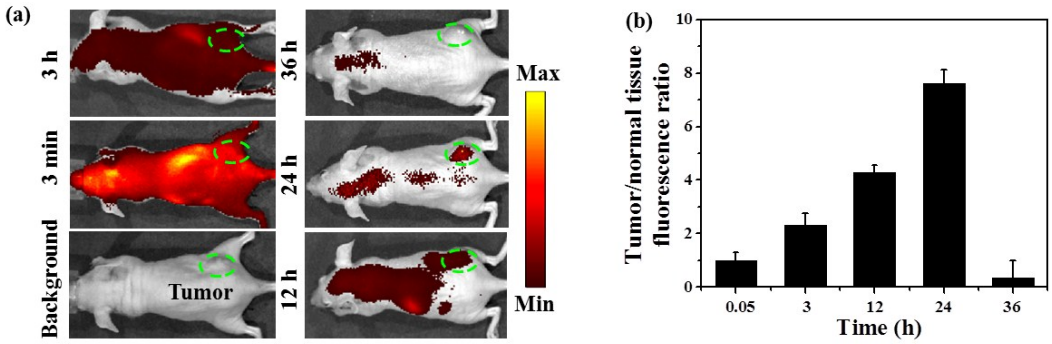

Figure S11 (a) Fluorescence images of tumor bearing mice at 3 min, 3h, 12h, 24h, 36h post intravenous injection of sMoSe$_2$-ICG NSs. (b) Statistical results of fluorescence signals in the tumor region over time. PA: photoacoustic, US: ultrasound.

Figure S12

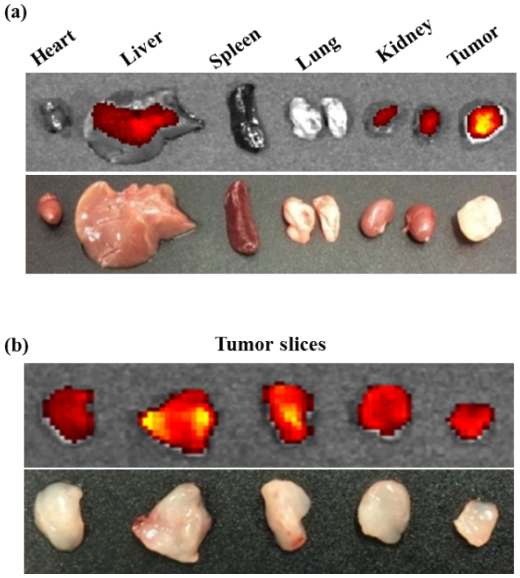

Figure S12 Fluorescence images of (a) major organs and (b) tumor slices from sMoSe$_2$-ICG NSs injected tumor bearing mice at 24 h point.